JMBFS

Journal of Microbiology, Biotechnology and Food Sciences

International peer-reviewed scientific online journal

Published by Faculty of Biotechnology and Food Sciences

PRELIMINARY INVESTIGATION INTO PROSPECTIVE APPLICATIONS OF NANOSILVER, PRODUCED USING TEFF (*Eragrostis tef*) FLOUR EXTRACT

Rocktotpal Konwarh[1,2], Abie Workie[1], Abyalew Moges[1], Daniel Seifu[1], Dereje Elias[1], Nahil Kebede[1], Yosef Tsigemariam[1], Anand Pratap Singh[2,3]*

Address(es):
[1] Department of Biotechnology, Addis Ababa Science and Technology University, Kilinto, Addis Ababa, 16417, Ethiopia.
[2] Baba Kinaram Research Foundation, 769/1-A, Brahmsthan, Sahadatpura, Mau, Uttar Pradesh, 275101, India.
[3] Center for Multidisciplinary Research, Tezpur University, Napaam, Sonitpur, Assam, 784028, India.

*Corresponding author: rock1311@gmail.com, rocktotpal.konwarh@aastu.edu.in

https://doi.org/10.55251/jmbfs.9892

ARTICLE INFO

Received 13. 2. 2023
Revised 17. 1. 2024
Accepted 31. 1. 2024
Published 1. 4. 2024

Regular article

OPEN ACCESS

ABSTRACT

Silver-based nanomaterials have etched an indelible mark in multiple domains. The green synthesis of silver nanoparticles has received significant attention over the last few years *vis-à-vis* the conventional use of toxic chemicals and reagents in the preparatory stages. In this milieu, the work reported here highlights the use of an aqueous extract of teff (*Eragrostis tef*) flour to prepare silver nanoparticles (TSNPs). The compositional abundance of various phytochemicals, sunlight-induced bio-reduction of silver ions, and subsequent stabilization of the nanostructures by teff's biomolecules were adroitly exploited. UV-visible spectroscopic analysis was employed to track the evolution of the TSNPs over time and their month-long storage stability. Exhibiting λ_{max} at around 426 nm and energy gap (as revealed by Tauc's plot) of 2.26 eV, the silver nanomaterial was employed for methylene blue dye degradation (50% degradation in less than 20 min) and DPPH scavenging (IC_{50} = 243.42 µL containing 410 µg of TSNPs), attesting their catalytic and anti-oxidant potency. On the other hand, anticoagulant action and a concentration-dependent variation were noted for radicle length post germination of *Cicer arientinum* seeds, treated with the TSNPs. The TSNPs could have profound implications in multiple domains.

Keywords: Silver nanoparticles, Teff, UV-visible spectroscopy, DPPH scavenging, Dye-decolorization, Anticoagulant, Phyto-compatibility

INTRODUCTION

In the quest for sustainable and eco-friendly approach for the fabrication of nanoparticles and other nanoscale structures, green synthesis harnesses the power of biological and renewable entities, such as plants, microorganisms, or enzymes, to produce nanomaterials (**Konwarh *et al.*, 2010; Konwarh *et al.*, 2011, Bachheti *et al.*, 2019; Alsaiari *et al.*, 2023; Dogra *et al.*, 2023**). Unlike the conventional slow and costly methods that entail toxic chemicals and energy-intensive processes, resulting in polydisperse, unstable nanoparticles with requisite for additional capping agent (**Kaabipour and Hemmati, 2021**), the greener fabrication protocols primarily involve water as the reaction medium and/or other green chemistry approaches/tools such as green eutectic solvents (**Nam *et al.*, 2023**), sono-chemical approach (**Joshi *et al.*, 2023**) and microwave irradiation (**Kaur *et al.*, 2023**). Such green methods are envisaged to reduce the environmental footprint besides offering advantages, including cost-effectiveness and the ability to control particle size and shape, although, structural and functional complexity of nanomaterials, fabricated using greener routes demand deeper delving (**Santo-Orihuela *et al.*, 2023**). The potential use of green-synthesized nanomaterials spans across diverse domains, from medicine and catalysis to environmental remediation and sustainable energy solutions, driving the development of a future based on cleaner and sustainable technological applications (**Rani *et al.*, 2023; Sani *et al.*, 2023; Ramezani Farani *et al.*, 2023**). Amongst others, the recent use of various phytoextracts, such as *Terminalia paniculata* Roth based antioxidant and anti-inflammatory silver nanoparticles (**Vernekar and Taranath, 2023**); banana pith extract based antibacterial and catalytic gold nanoparticles (**Nayak *et al.*, 2018**); *Syzigium cumini* leaf extract based iron oxide nanoparticles for prospective nano-biofertilizer applications for optimizing legume production (**Saleem and Khan, 2023**); and *Moringa oleifera* extract based copper oxide nanoparticles for energy storage applications (**Ikhioya *et al.*, 2023**) etc. merits special mention.

Teff (*Eragrostis tef*), the annual cereal grass (family Poaceae), grown for its tiny nutritious seeds is native to Ethiopia and Eritrea and serves as a staple food crop to millions of people. The recognition that teff is gluten-free has instigated tremendous research impetus in the food science domain (**Homem *et al.*, 2022; Girija *et al.*, 2022**). Consequently, scientific documentation on the nutritional composition, processing quality, and health benefits of teff is pacing up. The existing literature suggests that teff is composed of complex carbohydrates with slowly digestible starch. Teff has a similar protein content to other more common cereals like wheat, but is relatively richer than the latter in the essential amino acid, lysine. It is also a good source of essential fatty acids, fiber, minerals (especially calcium and iron), and phytochemicals such as polyphenols and phytates (**Baye, 2014; Zhu, 2018; Girija *et al.*, 2022; Yisak *et al.*, 2022**). Pertinently, the compositional abundance of such biomolecules may be suitably exploited as prospective bio-reductant and stabilizing agent in the green synthesis of nanomaterials such as silver nanoparticles. Till date there exists very few reports on the use of teff in the domain of nanotechnology. High temperature and toxic reagents like H_2SO_4 and HCl have been used to prepare nanosilica from teff straw (**Bageru *et al.*, 2017**). Similarly, response surface methodology (RSM) has been resorted to prepare teff straw-based silica nanoparticles in a recent work (**Amibo *et al.*, 2022**). On the other hand, **Bacha and Demsash (2021)** had reported the extraction of nanocellulose from teff straw using hot water treatment, acid-chlorite delignification, and alkaline hydrolysis process. Barring this, not much has been delved into the use of this extremely prospective bioresource for nanotechnological applications in accordance to the dictates of 'green nanotechnology' which focuses on resorting to preparation of nanomaterials under ambient conditions, use of less toxic reagents and lesser energy expense besides water as the reaction medium, as highlighted in the introductory section.

Dictated by the afore-stated information, we proposed to develop an environmentally benign approach using water as the solvent and exploitation of the various biomolecules in aqueous extract of teff for the preparation and stabilization of silver nanoparticles (TSNPs) for a range of applications. This stems from the following hypothesis: Teff seeds (**Baye, 2014**) are a source of both bound and free polyphenols such as catechin, ferulic, rosmarinic, protocatechuic, p-coumaric acids as well phytosterols and vitamins. High abundance of proteins, carbohydrates, fibers, and other minerals has been documented. The compositional abundance of various polyphenolic compounds and biomacromolecules in the aqueous extract of teff powder could be bracketed together with its plausible bio-reductive potency to generate silver nanoparticles from silver salt as well as endowing of electrostatic and steric stability to the nanoparticles. Furthermore, a high surface to volume ratio of the prepared nanoparticles is envisaged, implying a highly active surface (dictated by shape-size-surface chemistry accord) could be exploited for multiple applications like catalysis etc.

MATERIALS AND METHODS

Teff based aqueous extract mediated reduction

3 g white teff flour (procured from local market), suspended in 100 mL of double distilled water was subjected to overnight stirring over a magnetic stirrer (the ambient temperature was ~25 ºC) and subsequent filtration through a muslin cloth to prepare teff based aqueous extract. Aqueous solution of silver nitrate ($AgNO_3$) (Abron Chemicals, India) was subjected to reduction using the teff extract, added drop by drop, followed by gentle manual swirling of the contents in conical flasks (replicates of three for various experimental conditions). The reaction was carried out in (a) a dark-chamber (the ambient temperature was ~23 ºC), (b) under ambient light of the laboratory (the ambient temperature was ~24.5 ºC) and (c) under sunlight (the ambient temperature was ~30 ºC), using the reducing agent and the silver nitrate solution, adjusted to different v/v ratios (1:1, 1:2. 2:1) while the variations in the molarity of the silver nitrate solution were 0.01, 0.02, and 0.03 M. Monitoring the rapidity of visible color-change (indicating the reduction of the silver ions and consequent formation of nanoparticles) and UV-visible spectral analysis assisted in choosing the reaction-conditions (dictated by the objective of preparing nanoparticles with narrow-size distribution/ lesser polydispersity). These initial studies had dictated us to select the parameters of 2:1 (v/v) reducing agent: silver salt (0.01 M) solution for the preparation of the nanoparticles under sunlight. The results reported in this work are for the nanoparticles prepared under these parameters.

UV-visible spectroscopic characterization

The time-course dependent formation as well as a month-long dependent storage stability of the TSNPs were monitored using BIOCHROM Libra UV-visible double-beam spectrophotometer (scanning range: 300-700 nm, path length: 10 mm, bandwidth: 1 nm, single- cycle). Tauc's plot was used to calculate the band gap energy of the TSNPs. All the graphs were plotted and analyzed using the OriginPro 8 software.

Dye decolorization test (to check the prospective application as catalyst)

1 mg of methylene blue (MB) (Abron Chemicals, India) was dissolved in 100 mL of distilled water and its absorbance was monitored spectrophotometrically. The experiment was conducted by adding 1 mL of freshly prepared 0.2 M $NaBH_4$ (SRL Chemicals, India) to 25 mL aqueous solution of MB at room temperature (~25 ºC). To this 1 mL of TSNPs was added and the reactants were vortexed. At a regular interval of time, 250 µL of the reaction mixture was withdrawn and diluted with 2.75 mL distilled water. The absorption of the mixture was monitored periodically using UV–visible spectrophotometer. The degradation was also monitored without the TSNPs. The reaction kinetics were evaluated by assuming the concentration of reactive dyes obeying the pseudo-first order reaction, where the integrated form is expressed as follows:

$$\ln A_t/A_0 = - kt \quad \ldots[1]$$

where, A_0 is the absorbance at zero time, A_t is the absorbance at time *t*, and *k* is the rate constant

DPPH scavenging test (to check the prospective application as anti-oxidant)

Antioxidant activity of the TSNPs was measured by using the modified DPPH method as reported previously (**Konwarh *et al.*, 2011**). To examine the anti-oxidant potency, 200 µL, 400 µL, 600 µL, 800 µL and 1000 µL of the TSNPs were mixed with 2 mL of 100 µM DPPH (SRL Chemicals, India) solution. The samples were vortexed for around 15 s and allowed to scavenge DPPH in dark for 30 min. The absorbance of the samples was measured at 517 nm. In all the cases, measurements were done in triplicates. The scavenging percentage was calculated using the formula:

$$\text{DPPH scavenging} = \{(A_C - A_S)/A_C\} \times 100 \quad \ldots[2]$$

where A_C and A_S are absorption of blank DPPH and DPPH subjected to interact with the TSNPs at 517 nm, respectively.

Anticoagulant activity assessment

The experimental protocol to test the anticoagulant activity of the TSNPs was adopted from previously published report (**Raja *et al.*, 2015**). Briefly, blood was collected from a healthy volunteer (post receipt of appropriate written consent) in different vials (C, S, T) without any anticoagulant by medical personnel, stationed at AASTU health-center. Immediately, TSNPs and teff extract were added to the tube S and T respectively at 0.5% (v/v) and anticoagulant activity of the samples was assessed. EDTA-tube (marked as E) served as positive control while vial C served as negative control. This experiment was approved by the B.Sc. Project Proposal Evaluation Committee, Department of Biotechnology, AASTU.

Effect on seed germination (Phyto-compatibility assessment)

Assessing the phytotoxicity of nanoparticles (**Konwarh *et al.*, 2011**) was our next objective. For this, *Cicer arientinum* (chick pea) seeds were procured from the local market. The average germination rates of the *Cicer arientinum* seeds were greater than 95% as revealed in our initial experimentation. Seeds were kept in a dry and dark place at room temperature before use. These were surface sterilized in 1:1 volume of 3% hydrogen peroxide (SRL Chemicals, India) for 10 min, followed by rinsing thrice with distilled water. About 15 seeds were then soaked in distilled water (control) or nanoparticle suspension, taken in different concentrations for about 12 h. The soaking process resulted in imbibition and consequent swelling in all the seeds. The water and the nanoparticles suspension were drained off post soaking. The seeds were then, placed (with sufficient distance between each seed) on a piece of cotton filter-cloth (10 cm x 10 cm), taken on a Petri dish. The Petri dishes were incubated in the dark for 3 days (room temperature: ~ 26.5 ^{0}C). Number of seeds germinated for each treatment as well as the length of the emanating radicles were noted. The experiment was conducted in replicates of three and the results were expressed as mean ± standard deviation. In conjunction to the above tests, the seeds were also soaked and incubated in the aqueous teff extract.

RESULTS AND DISCUSSION

Preparation and UV-visible spectroscopic analysis

In the present study, the first objective was to use the aqueous extract of teff flour to prepare the TSNPs. The optical properties of nanoparticles are sensitive to size, shape, concentration, agglomeration state, and refractive index near the nanoparticle surface, therefore, UV-visible/IR spectroscopy serve as tools of immense pertinence in identifying and characterizing these materials. The UV-visible spectra supported the successful green-route mediated generation of the silver nanoparticles. No absorption peak was observed in UV-visible spectrum of Ag^+ solution before reduction (**Figure 1**). This is attributed to Ag^+ ions' d^{10} configuration (**Konwarh *et al.*, 2011**).

In our pursuit to 'go green' we had resorted to the use of sunlight as catalyst for the generation of the nanoparticles. Initially, we had tried to reduce the silver salt under (a) dark condition and (b) ambient light condition of the laboratory at room temperature. Although, there was visible color change (colorless to yellow, indicative of the reduction of the silver salt), it took considerably a long time (more than an hour) in both the cases. For the photo-assisted preparation, the gradual generation of silver nanoparticles, using 2: 1 ratio of the reducing agent and silver nitrate solution, was indicated by the progressive increase (till 22 min) in the absorbance intensity at around 420-430 nm in the UV-visible spectra. This is attributable to silver's surface plasmon resonance (SPR) (**Figure 1**). The optical absorption of metal nanoparticles has been described traditionally and classically by Mie theory (**Mie, 1908**) as the localized surface plasmon resonance (LSPR). The optical absorption of metal nanoparticles can be described quantum mechanically due to intra- band excitations of conduction electrons by photon, mimicking the interactions of light on metal surface via the photoelectric absorption and Compton scattering. Plasmonic coupling of metal nanoparticles with light augments several useful optical phenomena that find application in ultra-sensitive biomolecular detection and lab-on-a-chip sensors. Furthermore, we had also assessed the prospects of preparing nanoparticles using solutions of varied ratios of the reducing agent and the silver salt. However, the preparation using 1:1 and 1:2 ratios required considerably long time and was associated with the appearance of a broad SPR peak, at around 450 nm, indicating considerably large particle size and polydisperse nanoparticles. Thus, we had resorted to proceed with the nanoparticles, prepared using 2:1 reducing agent to silver salt solution.

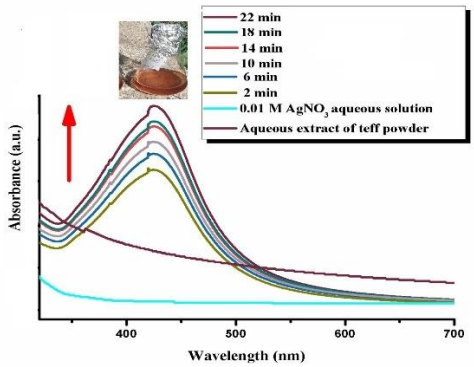

Figure 1 UV-vis spectra of the aqueous extract of teff flour, the aqueous solution of the silver salt, and the TSNPs that exhibit SPR at 426 nm. The evolution of silver nanoparticles over time is depicted.

The rapid generation of the silver nanoparticles under the influence of sunlight (photo-induced bio-reduction) could possibly be due to photo-induced homolytic

cleavage of the O-H bond of the various bio-reductants (example, amino acids) to form hydrogen radical that eventually transfers its electron to silver ion (Ag^+), generating silver nanoparticles. The oxygen radical part attains stabilization in the solution through extended conjugation. On the other hand, the compositional abundance of the biopolymers like starch in the teff extract is expected to confer steric stabilization to the nanoparticles (**Figure 2).**

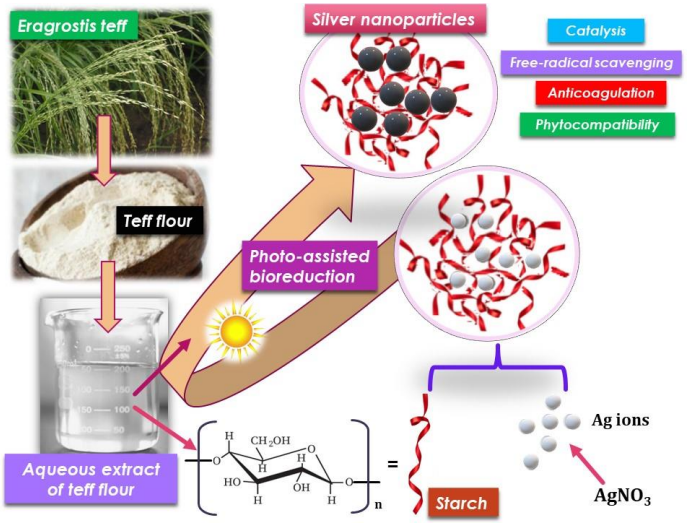

Figure 2 Schematic representation of photo-induced bioreduction of the silver ions based on the aqueous extract of teff flour and the subsequent generation of stable silver nanoparticles

Based on the UV-visible spectral analysis, we then proceeded with the calculation of the band gap in the prepared TSNPs. Nanoparticles are larger than individual atoms and molecules but are smaller than bulk solid. They obey neither absolute quantum chemistry nor laws of classical physics and have properties that differ markedly from those expected. The effect of size quantization particularly in metals and semiconductors is profound. The size of a nanoparticle is comparable to the *de Broglie* wavelength of its charge carriers (*i.e.*, electrons and holes). Due to the spatial confinement of the charge carriers, the edge of the valence and conduction bands split into discrete, quantized, electronic levels (**Figure 3**). These electronic levels are like those in atoms and molecules. The spacing of the electronic levels and the bandgap increases with decreasing particle size. This is because the electron hole pairs are now much closer together and the Coulombic interaction between them can no longer be neglected, giving an overall higher kinetic energy. This increase in bandgap can be observed experimentally by the blue-shift in the absorption spectrum or sometimes even visually by the color of the samples. A larger bandgap means that more energy is required to excite an electron from the valance band to the conduction band and hence light of a higher frequency and lower wavelength would be absorbed.

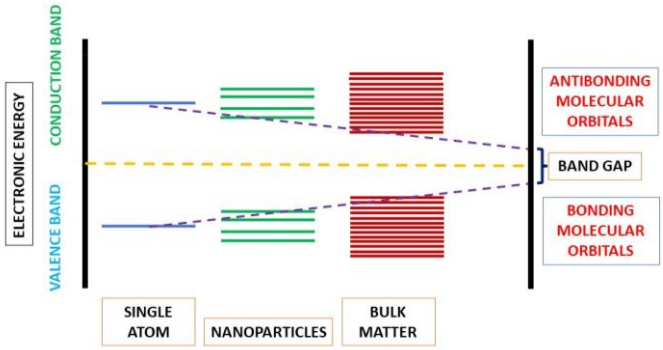

Figure 3 Band-gap change in nanoparticles

The maximum absorbance wavelength is associated with the conduction band energy according to quantum theory of metal nanoparticles (**Gharibshahi *et al.*, 2017**). The conduction band energy of Ag nanoparticles can be calculated indirectly from the absorption spectra by the following ***Tauc's equation***:

$$(\alpha h\nu)^2 = B(h\nu - E_{cb}) \qquad [3]$$

where α is the absorption coefficient, hν is the photon energy, E_{cb} is the conduction band energy, and B is a constant. According to this equation, by plotting the $(\alpha h\nu)^2$ versus energy and extrapolation of the linear part of the curve to the energy axis, the conduction band energy of Ag nanoparticles can be obtained as shown in **Figure 4**. The band gap for the TSNPs was calculated as 2.26 eV. This is quite high compared to bulk silver (0 eV) and in lines with previously reported values for nanoparticles (**Banerjee *et al.*, 2008; Yukna, 2007; Gharibshahi *et al.*, 2017**).

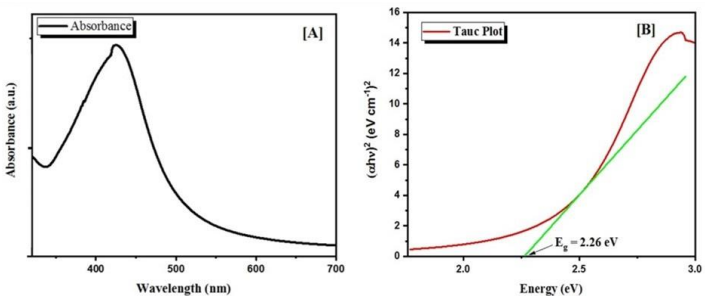

Figure 4 [A] UV-visible spectrum of the TSNPs, [B] Tauc plot, Variation of $(\alpha h\nu)^2$ with eV for Ag nanoparticles as a function of wavelength

We had also resorted to the UV-visible spectroscopic studies to understand the storage stability of the nanoparticles under room temperature (~23-26 ^{O}C). In our case, post storage of the TSNPs for a month, a slight shift of SPR peak (from 426 nm to 430 nm) was observed, however, the peak width remained the same (**Figure 5**). The biomolecules present in the teff flour extract were envisaged to act both as the reducing and stabilizing agent, thereby preventing excess aggregation of the nanoparticles. It is pertinent to note that scattering from a sample is typically highly sensitive to the aggregation state of the sample, with scattering contribution augmenting with the increase in the aggregation of the particles.

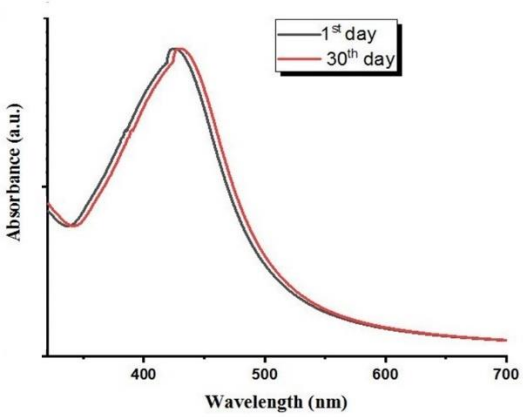

Figure 5 UV-visible spectra demonstrating the considerable stability of the nanoparticles, stored under ambient conditions over a month

The optical attributes of nanoparticles may be altered when particles aggregate and the conduction electrons (as in silver nanoparticles) near each particle surface become delocalized and are shared amidst the neighboring particles. Occurrence of such events leads to shifting of the SPR to lower energies, causing the absorption and scattering peaks to exhibit red-shift to longer wavelengths.
(Due to inaccessibility of other characterization tools (DLS, zeta potential, HRTEM etc.) during the execution of this B.Sc. project work in Ethiopia, we could not present a complete landscape of the physicochemical characterization of the nanoparticles. Nevertheless, the UV-visible spectroscopic analysis attested or at least indicated the successful preparation of the TSNPs. Thus, we proceeded with our investigation into their prospective applications and preliminary delving of their action at the bio-interface.)

Dye decolorization (application as catalyst)

Use of various dyes in paper, plastic, leather, food, cosmetic and textile industries have led to multiple issues including skin irritation, liver, kidney damage as well as the widespread application could prove detrimental to the central nervous system and even result in mutation and cancer (**Latha *et al.*, 2019**). The need of the hour is to mitigate the various synthetic dyes economically and safely in the environment. Amongst others, techniques such as carbon sorption, redox treatment, phyco-remediation, UV-light mediated degradation etc., have been explored (**Latha *et al.*, 2019**). Use of nanoparticles for dye-abatement (**Fairuzi *et al.*, 2018**) has been proposed as a rapid, low-cost methodology (without the formation of polycyclic products and oxidation of pollutants). In this regard, we had resorted to test the efficacy of the TSNPs for decolorization of methylene blue (MB), a common cationic dye. We found that the TSNPs functioned as an efficient catalyst (**Figure 6 [A]**) in decolorizing aqueous MB in presence of $NaBH_4$. The decrease of absorbance at λ_{max} (664 nm) of MB with time was followed spectrophotometrically. The bar diagram depicts the percentage of MB degradation with exposure time (**Figure 6 [B]**).

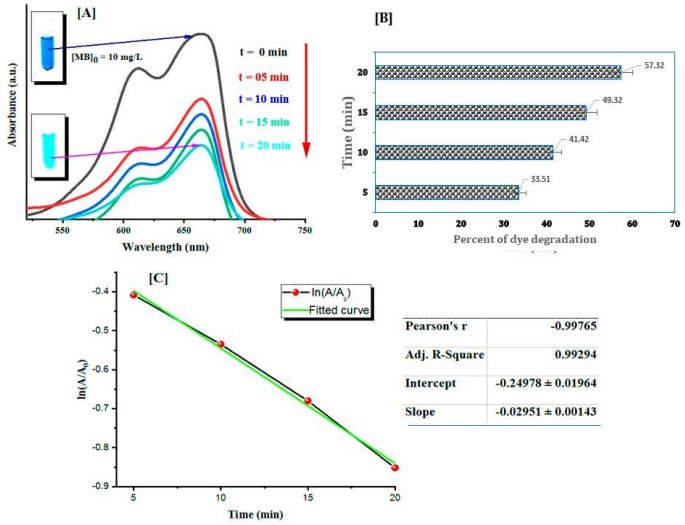

Figure 6 [A] Time-course-dependent absorption spectra of the MB solution in the presence of the TSNPs. [B] Percentage of dye degradation with respect to time [C] Kinetics of MB decolourization by the TSNPs

The degradation-percentage (%) of the dye was calculated by using the formula:

$$\text{Dye degradation (\%)} = \{(A_0 - A/A_0)\} \times 100 \quad \ldots[4]$$

where, A_0 is the initial concentration of MB solution and A is the concentration after *t* minutes of reaction.

In the absence of the nanocatalyst, the dye-decolorization was found to the negligible. Addition of the nanoparticles resulted in more than 50% decolorization in less than 20 min. The kinetic data were fitted to first order rate equations value (**Figure 6 [C]**). The nanoparticles are envisaged to act as electron relay and initiate shifting of electron from BH^{4-} ion (donor B_2H_4/BH_4^-) to acceptor (acceptor LMB/MB), leading to reduction of the dye. Concomitant adsorption of the BH^{4-} ion on the surface of the nanoparticles is followed by electron transfer from the BH_4^- ion into the dye via the nanoparticles (**Kumari *et al.*, 2015**). Highlights of a few studies on MB dye degradation using silver nanoparticles, fabricated using phyto-extracts are presented in **Table 1**.

DPPH scavenging (application as anti-oxidant)

The free radical scavenging of the TSNPs was evaluated in the present study. The percent scavenging of DPPH increased almost linearly with the increase in the concentration of the nanoparticles in the test samples (**Figure 7**). From the plot, 50% DPPH scavenging was calculated for 243.42 µL of the TSNPs. Previously, **Lalsangpuii *et al.* (2022)** had reported that the DPPH scavenging activities of AgNPs, prepared using *Spilanthes acmella* leaf extract (IC_{50}: 3.85 ± 0.04 µg/mL) was significantly higher than that of *S. acmella* leaf extract (SAAE) (IC_{50}: 474.0 ± 8.80 µg/mL). On the other hand, AgNPs, fabricated using spice blend of garlic, ginger and cayenne pepper exhibited greater inhibition of DPPH radical with IC_{50} < 31.25 µg/mL against 68.75 µg/mL for 2,2′-azinobis (3-ethylbenzothiazoline-6-sulfonic acid) or ABTS (**Otunola and Afolayan, 2018**). IC_{50} values of 385.87 µg/mL and 30.04 µg/mL for DPPH scavenging was recorded for AgNPs, prepared using aqueous extract of silk hair of corn (**Patra and Baek, 2016**) and *Erythrina suberosa* (Roxb.) (**Mohanta *et al.*, 2017**) respectively. Recent work has unmasked IC_{50} values of 82 ± 0.079, 44.56 ± 0.02 and 26.6 ± 0.06 µg/mL corresponding to flaxseed extract, AgNPs, fabricated using flaxseed extract, and ascorbic acid respectively (**Alzubaidi *et al.*, 2023**). Previously, the corresponding author of this work had also reported DPPH based antioxidant activity of *Colocasia esculenta based* silver nanoparticles (**Barua *et al.*, 2013**) besides free radical scavenging using orange peel-based silver nanoparticles (**Konwarh *et al.*, 2011**). Numerous anti-oxidants of the orange peel (pooled into the system during preparation and consequently surface-adsorbed) were proposed to act synergistically in that system. Furthermore, with a high surface area to volume ratio and an ambient electrostatic field with anti-oxidant bio-moieties on the surface, these silver nanoparticles were anticipated to develop a high tendency to interact with and reduce DPPH like species. In this work, although, a higher volume was required for our sample (in comparison to previous work, as reported by **Konwarh *et al.* (2011)**, possibly due to lesser abundance of polyphenolic compounds in teff compared to orange peel) to display 50% scavenging, nevertheless, it raises the prospects of incorporating the prepared nanoparticles for developing of nanocomposite packaging materials with the facet of free radical scavenging. The nano-chemistry involved in this free radical scavenging attribute of the nanoparticles needs further investigation, besides appropriate dilutions and concentrations are important aspects in anti-oxidant assays.

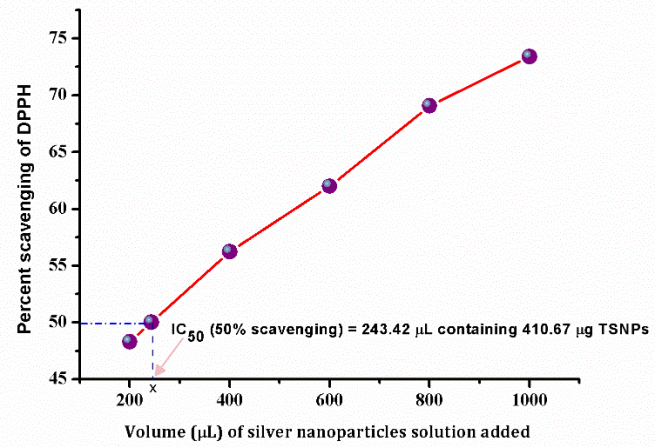

Figure 7 DPPH scavenging activity of the silver nanoparticles

Table 1 Few comparative results on the studies on MB dye degradation using silver nanoparticles, fabricated using phyto-extracts

Phytoextract/bioresource used for Ag NP preparation	Highlights about MB degradation	Reference
Morinda tinctoria leaf extract	Degradation efficiency percent of AgNPs was registered as 95.3% at 72 h	Vanaja *et al.* (2014)
Trigonella foenum-graecum seeds extract.	Complete reduction of MB to leucomethylene blue (LMB) was accomplished in less than 20 min in the presence of AgNPs	Vidhu and Philip (2014)
Polygonum hydropiper extract	The MB solution turned into colourless solution within less than 15 min under UV light and vigorous stirring conditions	Bonnia *et al.* (2016)
Convolvulus arvensis leaf extract	Reduction of MB within 20 min in the presence of AgNPs with rate constant of 0.108 min^{-1}	Hamedi *et al.* (2017)
Nepeta leucophylla stem extract	Photocatalytic degradation of MB using biosynthesized silver nanoparticles of optimized dose (1.8 mL) for 180 min in the presence and absence of light were 82.8% and 61.25%, respectively	Singh and Dhaliwal (2018)
Brassica oleracea var. *Botrytis* waste extract	Maximum MB dye degradation of 97.57% was recorded at 150 min	Kadam *et al.* (2020)
Coleus vettiveroids leaf extract	Degradation of organic dyes (including MB) within 3 hours of exposure time in presence of sunlight.	Ajay *et al.* (2022)
Syzygium samarangense flower extract	Within 2 h of direct sunlight, a maximum of 80% photocatalytic degradation of MB was reported	Basalius *et al.* (2023)
Onobrychis sativa extract of leaves and flowers mixture	The catalytic degradation of MB by $NaBH_4$ in the presence of AgNPs@Os was found to be 68 % in 30 min.	Erenler and Hosaflioglu (2023)
Eragrostis tef extract	50% decolourization in less than 20 min	This study

Anticoagulant activity

Assessment of hemocompatibility of silver nanoparticles has been a prime focus in the realm of nanotoxicity assessment. Amongst others, **Krajewski *et al.* (2013)** pointed out that silver nanoparticles, on contact with blood could modulate the coagulation cascade (the sequence of various biochemical events involved in coagulation) or the inflammatory response. **Shrivastava *et al.* (2009)** had proved the potential of antiplatelet and antithrombic effect of silver nanoparticles and concluded that the silver nanoparticles have innate antiplatelet property which prevents integrin-mediated platelet responses. **Kim *et al.* (2013)** demonstrated that the anticoagulant property of heparin was enhanced by the addition of earthworm extract mediated gold nanoparticles. In our study, the anticoagulant property of TSNPs was examined by the addition of TSNPs to freshly collected blood (**Figure 8**). Blood clot was observed in the tube without any anti-coagulant. Blood collected in the EDTA-tube served as the control. On the other hand, no clot was observed for the blood collected in vials, supplemented with the TSNPs. This confirmed that the TSNPs could serve as blood anticoagulant. This is in accordance with the results obtained by **Jeyaraj *et al.*, (2013)** and **Raja *et al.*, (2015)**. However, the effect of the nanoparticles on the morphology, population and functionality of the various blood cells must be studied in details.

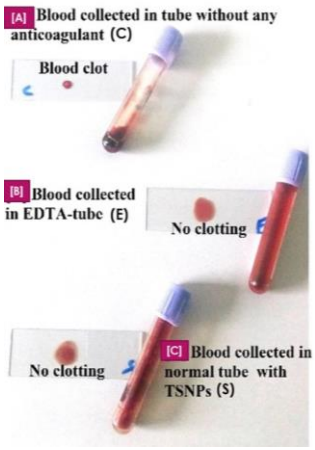

Figure 8 Anticoagulant activity assessment of the TSNPs on blood collected freshly from a healthy volunteer

Effect on seed germination (Phyto-compatibility assessment)

Exotics like nanoparticles can penetrate via the cell wall, primarily composed of polymeric carbohydrates, prior to membrane invagination in plant cells (**Konwarh *et al.*, 2011**) and can lead to alteration in various physiological activities of the plants. In this backdrop, investigation of the modulation of the phyto-physiology, assessed in terms of seed germination due to the plausible penetration of the TSNPs was one of the propositions in this work (**Figure 9**). Plant seeds with emerging radicle or cotyledon coming out of the seed coat were recorded as being germinated in the present experiment.

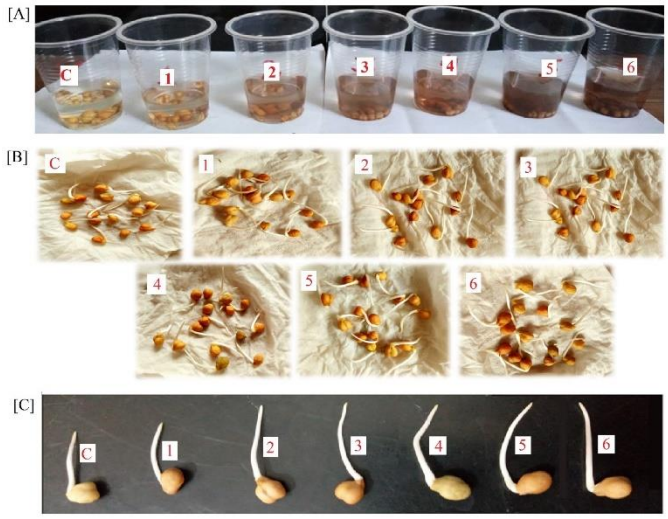

Figure 9 [A] Treatment of *Cicer arientinum* seeds with different concentrations of TSNPs [B] Representative batch of germinated seeds, post three days of treatments [C] Representative seeds with emanating radicles. Here, C refers to the control (without any treatment), while for codes 1-6, readers are requested to refer to Table 2

In our experiment, it was observed that the average germination rate remained unchanged for the treated seeds with respect to the control. However, significant difference was noted for the average radicle length post four days of incubation (**Table 2**).

Table 2 Phytotoxicity assessment of the TSNPs - on germination and radicle length of *Cicer arientinum*

Sample	Average germination rate (%) of the seeds	Average radicle length (cm) post four days of incubation
Control (*Sample code: C*)	98%	2.1 ± 0.3
TSNPs (25 µL in 50 mL distilled water, resulting in final concentration of 0.84 µg/mL TSNPs) (*Sample code: 1*)	100%	2.3 ± 0.2
TSNPs (100 µL in 50 mL distilled water, resulting in final concentration of 3.36 µg/mL TSNPs) (*Sample code: 2*)	100%	3.6 ± 0.3
TSNPs (200 µL in 50 mL distilled water, resulting in final concentration of 6.72 µg/mL TSNPs) (*Sample code: 3*)	98%	4 ± 0.2
TSNPs (300 µL in 50 mL distilled water, resulting in final concentration of 10.08 µg/mL TSNPs) (*Sample code: 4*)	99%	4.4 ± 0.2
TSNPs (400 µL in 50 mL distilled water, resulting in final concentration of 13.44 µg/mL TSNPs) (*Sample code: 5*)	100%	4.6 ± 0.2
TSNPs (500 µL in 50 mL distilled water, resulting in final concentration of 16.8 µg/mL TSNPs) (*Sample code: 6*)	99%	4.4 ± 0.1

At this juncture we would like to mention that a handful of recent studies has evinced that the innovative technique of nano-priming involving seed priming/treatment with nanomaterials enhances seed germination, growth, and yield while providing resistance to different plant stresses. The employed nanomaterials in the technique facilitate electron exchange and augmented surface interactions within plant cells and tissues. Events such as stimulation of rapid starch degradation through amylase activation, generation of nanopores in shoot, expression of aquaporin genes, assisting in water absorption, and triggering of reactive oxygen species (ROS)/antioxidant mechanisms in seeds leading to production of secondary metabolites and heightened stress tolerance have been projected in the context of the underlying mechanism (**Nile *et al.*, 2022**). To cite for evidence, seed priming using ZnO-NPs and 24-epibrassinolide (EBL), whether applied separately or together, resulted in improved seed germination and boosted the metabolic and homeostatic response in maize seeds cultivated under salt stress in comparison to the control group (**Alhammad *et al.*, 2023**). Similarly, **Acharya *et al.* (2020)** had reported that Ag NP-mediated seed priming resulted in better germination, growth, yield as well as maintained fruit quality in *Citrulllus lanatus* (watermelons). However, there exist contrasting reports on the phytomodulatory effects of different nanoparticles. **Shi *et al.* (2019)** had reported the germination-inhibitory effect of gold nanoparticles on mung-bean (*Phaseolus radiatus).* With increasing concentration of gold nanoparticles, chlorophyll and nitrogen contents in leaves decreased, superoxide dismutase (SOD), peroxidase (POD) and catalase (CAT) activities in both shoot and root increased first and then decreased, while the malondialdehyde (MDA) contents increased. On the other hand, at the end of 60 days of cultivation, **Timoteo *et al.* (2019)** documented that the *in vitro* germination of *Physalis peruviana* L. is not affected by the presence of AgNPs and that at low concentrations (0.385 mg/L) it can promote an increase in seedlings biomass. However, higher concentration (15.4 mg/L) was found to reduce the seedling size and root system, but no changes were observed in the seedlings' antioxidant metabolism and anatomy. On a contrasting note, various tested concentrations of AgNPs (10, 20, 40 ppm) were found to promote both the shoot and root growth which was evident from the increased length and biomass of rice seedlings (**Gupta *et al.*, 2018**). Exposure to AgNPs was also found to significantly increase the chlorophyll a and carotenoid contents. The molecular basis of these observation needs further investigation.

Cicer arietinum L., a dicotyledonous plant was chosen to assess the preliminary phytotoxicity of the prepared silver nanoparticles in this work. *C. arientinum* L. or chick pea, an important pulse crop (**Madurapperumage *et al.*, 2021**) acts as a great source of protein, fats and carbohydrates besides serving as a green manure and fodder for animals. It is readily accessible and manageable, capable of being

cultivated throughout the year and tolerant to a wide range of environmental changes. Additionally, it exhibits convenient germination with its thin seed coat. Pertinently, **Candan *et al.* (2022)** reported the application of infrared spectral analysis, aided by machine learning techniques to unveil that gold nanoparticles (AuNPs) and single-walled carbon nanotubes (CNTs) are taken up by *C. arietinum* seedlings' root, leading to consequent build-up of the nanomaterials in stem and leaf parts. Priming *Cicer arientinum* seeds with ZnO NPs (synthesized using *Trichoderma harzianum*) was projected as a means to aid chick pea plants to pile up greater amounts of sugars, phenol, total proteins, and superoxide dismutase (SOD) to resist wilt pathogen- *Fusarium oxysporum* (**Farhana *et al.*, 2022**). Similar protective action of treatment with AgNPs (biosynthesized by rhizopheric microflora of chick pea) against wilt disease was previously reported by **Kaur et al. (2018)**. Furthermore, AgNPs, synthesized using *Aloe vera* leaf extract (**Anju, 2022**) supported significant increment in biomass, shoot, and root growth in *C. arientinum* L. On the other hand, biosynthesized iron oxide nanoparticles (IONPs) have been found to support callus induction, shoot regeneration and root induction of chickpea plants for prospective application in plant tissue culture (**Irum *et al.*, 2020**). **Pawar *et al.* (2019)** had also assessed the impact of iron oxide nanoparticles (Fe_2O_3 NPs) on chickpea seedling growth using different concentrations (4-16 µg/mL). They found that lower concentrations (up to 12 µg/mL) enhanced seed germination and growth, but higher concentrations were inhibitory. Our preliminary investigation has shown that TSNPs do have a phyto-physiology modulatory effect, as reflected in the varied lengths of the emerging radicle. It is to be noted that the aqueous teff extract did not influence the seed-germination negatively and the results were in lines parallel to that of the control. As far as this study is concerned, besides delving into the effect on the shoot length and survival percentage of the seedlings post transplantation, a number of questions have to be addressed: Will the effect of the prepared samples and the consequences of the internalization and bio-distribution be same for both dicot and monocot plants? Is the phyto-modulatory action species-specific? Does the penetration of Ag NPs into the root cells help the plants to ward off soil pathogens or lead to the loss of beneficial microflora, peripheral to the roots?

CONCLUSION

This work mirrors the successful sunlight-assisted rapid and efficient biogenic synthesis of silver nanoparticles using aqueous teff powder extract (without any additional toxic chemicals), for multiple applications. However, the complete physicochemical attributes of the nanoparticles have not been investigated. The work reported in this work brings the fact to light that a common raw material of the Ethiopian food- delicacy can be useful even in the domain of nanotechnology. The stabilized silver nanoparticles synthesized under the ambient conditions shows tremendous potential for applications in several realms. These nanoparticles endowed with the attributes of free radical scavenging, catalysis, and anticoagulant potency as well as phyto-compatibility (as revealed in preliminary investigations) may be exploited for various biomedical, agricultural, and industrial applications. Furthermore, probing into the nano-biointerfacial actions at various levels could be the focus of future study. To cite for evidence, effect of the silver nanoparticles on PCR amplification of genes of interest, antimicrobial potency as well as *in vivo* effects could be investigated.

DECLARATION

(a) The un-reviewed version of this research article (with DOI: https://doi.org/10.21203/rs.3.rs-2595604/v2) is hosted as a preprint in Research Square since 23 Feb, 2023. The link to the article is https://www.researchsquare.com/article/rs-2595604/v2.
(b) The authors declare no conflict of interest.

Acknowledgments: A note of gratitude is forwarded to Addis Ababa Science and Technology University (AASTU), Ethiopia for supporting this B.Sc. project financially. The incessant support of the M.Sc. students (*Alazar Yeshitla, Bethelehem Getachew, Simatsidk Haregu, Setegn Haile and Abate Ayele*) merits special mention. A bouquet of gratefulness is extended to sister *Semeret G/Sellasie* for assisting in the anti-coagulant test at AASTU health centre.

REFERENCES

Acharya, P., Jayaprakasha, G. K., Crosby, K. M., Jifon, J. L., & Patil, B. S. (2020). Nanoparticle-mediated seed priming improves germination, growth, yield, and quality of watermelons (*Citrullus lanatus*) at multi-locations in Texas. *Scientific Reports*, *10*(1), 5037. https://doi.org/10.1038/s41598-020-61696-7

Ajay, S., Panicker, J. S., Manjumol, K. A., & Subramanian, P. P. (2022). Photocatalytic activity of biogenic silver nanoparticles synthesized using *Coleus Vettiveroids*. *Inorganic Chemistry Communications*, *144*, 109926. https://doi.org/10.1016/j.inoche.2022.109926

Alhammad, B. A., Ahmad, A., Seleiman, M. F., & Tola, E. (2023). Seed priming with nanoparticles and 24-epibrassinolide improved seed germination and enzymatic performance of *Zea mays* L. in salt-stressed soil. *Plants*, *12*(4), 690. https://doi.org/10.3390/plants12040690

Al-Zaban, M. I., Mahmoud, M. A., & AlHarbi, M. A. (2021). Catalytic degradation of methylene blue using silver nanoparticles synthesized by honey. *Saudi Journal of Biological Sciences*, *28*(3), 2007-2013. https://doi.org/10.1016/j.sjbs.2021.01.003

Alzubaidi, A. K., Al-Kaabi, W. J., Ali, A. A., Albukhaty, S., Al-Karagoly, H., Sulaiman, G. M., ... & Khane, Y. (2023). Green synthesis and characterization of silver nanoparticles using flaxseed extract and evaluation of their antibacterial and antioxidant activities. *Applied Sciences*, *13*(4), 2182. https://doi.org/10.3390/app13042182

Amibo, T. A., Beyan, S. M., & Damite, T. M. (2022). Production and optimization of bio-based silica nanoparticle from teff straw (*Eragrostis tef*) using RSM-based modeling, characterization aspects, and adsorption efficacy of methyl orange dye. *Journal of Chemistry*, *2022*, 1-15. https://doi.org/10.1155/2022/9770520

Anju, T. R. (2022). Phytotoxicity of Silver Nanoparticles on growth of *Cicer arietinum* L: A sustainable alternative using green synthesis. *ECS Transactions*, *107*(1), 799. https://doi.org/10.1149/10701.0799ecst

Bageru, A. B., & Srivastava, V. C. (2017). Preparation and characterisation of biosilica from teff (*Eragrostis tef*) straw by thermal method. *Materials Letters*, *206*, 13-17. https://doi.org/10.1016/j.matlet.2017.06.100

Bacha, E. G., Demsash, H. D. (2021). Extraction and characterization of nanocellulose from *Eragrostis* teff straw. Preprint (Version 1), available at *Research Square*. https://doi.org/10.21203/rs.3.rs-296990/v1

Bachheti, R. K., Konwarh, R., Gupta, V., Husen, A., & Joshi, A. (2019). Green synthesis of iron oxide nanoparticles: cutting edge technology and multifaceted applications, In: Husen, A., Iqbal, M. (Eds.) *Nanomaterials and Plant Potential*, 239–259. Springer, Cham. http://dx.doi.org/10.1007/978-3-030-05569-1_9

Banerjee, Arghya N., and Kalyan K. Chattopadhyay (2008) Reactive sputtered wide-bandgap p-type semiconducting spinel AB_2O_4 and Delafossite ABO_2 thin films for “Transparent Electronics." In Depla, D., Mahieu, S. (Ed.) *Reactive Sputter Deposition*. *Springer Series in Materials Science*, 109, 413-484. Springer, Berlin, Heidelberg. https://doi.org/10.1007/978-3-540-76664-3_12

Barua, S., Konwarh, R., Mandal, M., Gopalakrishnan, R., Kumar, D., & Karak, N. (2013). Biomimetically prepared antibacterial, free radical scavenging poly(ethylene glycol) supported silver nanoparticles as *Aedes albopictus* larvicide. *Advanced Science, Engineering and Medicine*, *5*(4), 291-298. https://doi.org/10.1166/asem.2013.1286

Basalius, H., Mani, A., Michael, A., Mary, S. M., Lenin, M., Chelliah, P., ... & Islam, M. A. (2023). Green synthesis of nano-silver using *Syzygium samarangense* flower extract for multifaceted applications in biomedical and photocatalytic degradation of methylene blue. *Applied Nanoscience*, *13*(6), 3735-3747. https://doi.org/10.1007/s13204-022-02523-5

Baye, K. (2014). Teff: nutrient composition and health benefits. ESSP Working Paper 67. Washington, D.C. and Addis Ababa, Ethiopia: International Food Policy Research Institute (IFPRI) and Ethiopian Development Research Institute (EDRI). http://cdm15738.contentdm.oclc.org/utils/getfile/collection/p15738coll2/id/128334/filename/128545.pdf

Bonnia, N. N., Kamaruddin, M. S., Nawawi, M. H., Ratim, S., Azlina, H. N., & Ali, E. S. (2016). Green biosynthesis of silver nanoparticles using *Polygonum hydropiper* and study its catalytic degradation of methylene blue. *Procedia Chemistry*, *19*, 594-602. https://doi.org/10.1016/j.proche.2016.03.058

Candan, F., Markushin, Y., & Ozbay, G. (2022). Uptake and presence evaluation of nanoparticles in *Cicer arietinum* L. by infrared spectroscopy and machine learning techniques. *Plants*, *11*(12), 1569. https://doi.org/10.3390/plants11121569

Dogra, S., Sharma, M.D., Tabassum, S., Mishra, P., Bhatt, A. K., Bhuyar, P. (2023). Green biosynthesis of silver nanoparticles (AgNPs) from *Vitex negundo* plant extract and its phytochemical screening and antimicrobial assessment next to pathogenic microbes. *Journal of Microbiology, Biotechnology and Food Sciences*, *12*(4), 1-7. http://dx.doi.org/10.55251/jmbfs.5993

Erenler, R., & Hosaflioglu, I. (2023). Green synthesis of silver nanoparticles using *Onobrychis sativa* L.: Characterization, catalytic degradation of methylene blue, antioxidant activity, and quantitative analysis of bioactive compounds. *Materials Today Communications*, *35*, 105863. https://doi.org/10.1016/j.mtcomm.2023.105863

Fairuzi, A. A., Bonnia, N. N., Akhir, R. M., Abrani, M. A., & Akil, H. M. (2018). Degradation of methylene blue using silver nanoparticles synthesized from *Imperata cylindrica* aqueous extract. In *IOP conference series: Earth and Environmental Science*, *105*, 012018. https://doi.org/10.1088/1755-1315/105/1/012018

Farhana, Munis, M. F. H., Alamer, K. H., Althobaiti, A. T., Kamal, A., Liaquat, F., ... & Attia, H. (2022). ZnO nanoparticle-mediated seed priming induces biochemical and antioxidant changes in chickpea to alleviate *Fusarium* wilt. *Journal of Fungi*, *8*(7), 753. https://doi.org/10.3390/jof8070753

Gharibshahi, L., Saion, E., Gharibshahi, E., Shaari, A. H., & Matori, K. A. (2017). Structural and optical properties of Ag nanoparticles synthesized by thermal treatment method. *Materials*, *10*(4), 402. https://doi.org/10.3390/ma10040402

Girija, A., Le Bihan, V., Wang, Z., Han, J., Yadav, R., & Mur, L. A. (2022). A phenomic-metabolomic pipeline for assessing the seed traits in the gluten free orphan cereal, *Eragrostis tef*. *Journal of Cereal Science*, *108*, 103573. https://doi.org/10.1016/j.jcs.2022.103573

Gupta, S. D., Agarwal, A., & Pradhan, S. (2018). Phytostimulatory effect of silver nanoparticles (AgNPs) on rice seedling growth: An insight from antioxidative enzyme activities and gene expression patterns. *Ecotoxicology and Environmental Safety*, *161*, 624-633. https://doi.org/10.1016/j.ecoenv.2018.06.023

Hamedi, S., Shojaosadati, S. A., & Mohammadi, A. (2017). Evaluation of the catalytic, antibacterial and anti-biofilm activities of the Convolvulus arvensis extract functionalized silver nanoparticles. *Journal of Photochemistry and Photobiology B: Biology*, *167*, 36-44. https://doi.org/10.1016/j.jphotobiol.2016.12.025

Hajra, A., & Mondal, N. K. (2017). Effects of ZnO and TiO_2 nanoparticles on germination, biochemical and morphoanatomical attributes of Cicer arietinum L. *Energy, Ecology and Environment*, *2*, 277-288. https://doi.org/10.1007/s40974-017-0059-6

Homem, R. V., Proserpio, C., Cattaneo, C., Rockett, F. C., Schmidt, H. D. O., Komeroski, M. R., Rios, A.D.O., Pagliarini, E & Oliveira, V. R. D. (2022). New opportunities for gluten-free diet: teff (*Eragrostis tef*) as fibre source in baking products. *International Journal of Food Science & Technology*, *57*(8), 4697-4704. https://doi.org/10.1111/ijfs.15395

Irum, S., Jabeen, N., Ahmad, K. S., Shafique, S., Khan, T. F., Gul, H., ... & Hussain, S. Z. (2020). Biogenic iron oxide nanoparticles enhance callogenesis and regeneration pattern of recalcitrant *Cicer arietinum* L. *Plos One*, *15*(12), e0242829. https://doi.org/10.1371/journal.pone.0242829

Jeyaraj, M., Varadan, S., Anthony, K. J. P., Murugan, M., Raja, A., & Gurunathan, S. (2013). Antimicrobial and anticoagulation activity of silver nanoparticles synthesized from the culture supernatant of *Pseudomonas aeruginosa*. *Journal of Industrial and Engineering Chemistry*, *19*(4), 1299-1303. https://doi.org/10.1016/j.jiec.2012.12.031

Kaabipour, S., & Hemmati, S. (2021). A review on the green and sustainable synthesis of silver nanoparticles and one-dimensional silver nanostructures. *Beilstein Journal of Nanotechnology*, *12*(1), 102-136. https://doi.org/10.3762/bjnano.12.9

Kadam, J., Dhawal, P., Barve, S., & Kakodkar, S. (2020). Green synthesis of silver nanoparticles using cauliflower waste and their multifaceted applications in photocatalytic degradation of methylene blue dye and Hg^{2+} biosensing. *SN Applied Sciences*, *2*, 1-16. https://doi.org/10.1007/s42452-020-2543-4

Kim, H. K., Choi, M. J., Cha, S. H., Koo, Y. K., Jun, S. H., Cho, S., & Park, Y. (2013). Earthworm extracts utilized in the green synthesis of gold nanoparticles capable of reinforcing the anticoagulant activities of heparin. *Nanoscale Research Letters*, *8*, 1-7. https://doi.org/10.1186/1556-276X-8-542

Konwarh, R., Gogoi, B., Philip, R., Laskar, M. A., & Karak, N. (2011). Biomimetic preparation of polymer-supported free radical scavenging, cytocompatible and antimicrobial "green" silver nanoparticles using aqueous extract of *Citrus sinensis* peel. *Colloids and Surfaces B: Biointerfaces*, *84*(2), 338-345. https://doi.org/10.1016/j.colsurfb.2011.01.024

Krajewski, S., Prucek, R., Panacek, A., Avci-Adali, M., Nolte, A., Straub, A., Zboril, R., Wendel, H.P., & Kvitek, L. (2013). Hemocompatibility evaluation of different silver nanoparticle concentrations employing a modified Chandler-loop *in vitro* assay on human blood. *Acta Biomaterialia*, *9*(7), 7460-7468. https://doi.org/10.1016/j.actbio.2013.03.016

Kumari, M. M., Jacob, J., & Philip, D. (2015). Green synthesis and applications of Au–Ag bimetallic nanoparticles. *Spectrochimica Acta Part A: Molecular and Biomolecular Spectroscopy*, *137*, 185-192. https://doi.org/10.1016/j.saa.2014.08.079

Lalsangpuii, F., Rokhum, S. L., Nghakliana, F., Fakawmi, L., Ruatpuia, J. V., Laltlanmawii, E., ... & Siama, Z. (2022). Green Synthesis of silver nanoparticles using *Spilanthes acmella* leaf extract and its antioxidant-mediated ameliorative activity against doxorubicin-induced toxicity in Dalton's Lymphoma Ascites (DLA)-bearing mice. *ACS Omega*, *7*(48), 44346-44359. https://doi.org/10.1021/acsomega.2c05970

Latha, D., Prabu, P., Gnanamoorthy, G., Sampurnam, S., Manikandan, R., Arulvasu, C., & Narayanan, V. (2019). Facile *Justicia adhatoda* leaf extract derived route to silver nanoparticle: synthesis, characterization and its application in photocatalytic and anticancer activity. *Materials Research Express*, *6*(4), 045003. https://doi.org/10.1088/2053-1591/aaf828

Madurapperumage, A., Tang, L., Thavarajah, P., Bridges, W., Shipe, E., Vandemark, G., & Thavarajah, D. (2021). Chickpea (Cicer arietinum L.) as a source of essential fatty acids–a biofortification approach. *Frontiers in Plant Science*, *12*, 734980. https://doi.org/10.3389/fpls.2021.734980

Mie, G. (1908) Contributions to the Optics of Turbid Media, Particularly of Colloidal Metal solutions. *Annalen der Physik*, *25*, 377-445. https://doi.org/10.1002/andp.19083300302

Mohanta, Y. K., Panda, S. K., Jayabalan, R., Sharma, N., Bastia, A. K., & Mohanta, T. K. (2017). Antimicrobial, antioxidant and cytotoxic activity of silver nanoparticles synthesized by leaf extract of *Erythrina suberosa* (Roxb.). *Frontiers in Molecular Biosciences*, *4*, 14. https://doi.org/10.3389/fmolb.2017.00014

Nile, S. H., Thiruvengadam, M., Wang, Y., Samynathan, R., Shariati, M. A., Rebezov, M., ... & Kai, G. (2022). Nano-priming as emerging seed priming technology for sustainable agriculture—recent developments and future perspectives. *Journal of Nanobiotechnology*, *20*(1), 1-31. https://doi.org/10.1186/s12951-022-01423-8

Otunola, G. A., & Afolayan, A. J. (2018). *In vitro* antibacterial, antioxidant and toxicity profile of silver nanoparticles green-synthesized and characterized from aqueous extract of a spice blend formulation. *Biotechnology & Biotechnological Equipment*, *32*(3), 724-733. https://doi.org/10.1080/13102818.2018.1448301

Patra, J. K., & Baek, K. H. (2016). Biosynthesis of silver nanoparticles using aqueous extract of silky hairs of corn and investigation of its antibacterial and anticandidal synergistic activity and antioxidant potential. *IET Nanobiotechnology*, *10*(5), 326-333 https://doi.org/10.1049/iet-nbt.2015.0102

Pawar, V. A., Ambekar, J. D., Kale, B. B., Apte, S. K., & Laware, S. L. (2019). Response in chickpea (*Cicer arietinum* L.) seedling growth to seed priming with iron oxide nanoparticles. *International Journal of Biosciences 14*(3), 82-91. http://dx.doi.org/10.12692/ijb/14.3.82-91

Raja, S., Ramesh, V., & Thivaharan, V. (2015). Antibacterial and anticoagulant activity of silver nanoparticles synthesised from a novel source–pods of *Peltophorum pterocarpum*. *Journal of Industrial and Engineering Chemistry*, *29*, 257-264. https://doi.org/10.1016/j.jiec.2015.03.033

Shi, X-M., Gao, C., Oiao, N-N., Wang, J-J., Zhu, J.M., Chen, Y-S., Cai, X-R, Xu, D-C, Wang, M-J, Xu, Z-D. (2019). Effects of gold nanoparticles on seed germination and seedling growth of mung bean (*Phaseolus radiatus*) and the underlying physiological mechanism." *Chinese Journal of Ecology 38*(4), 945-952. http://www.cnki.net/kcms/doi/10.13292/j.1000-4890.201904.038.html

Shrivastava, S., Bera, T., Singh, S. K., Singh, G., Ramachandrarao, P., & Dash, D. (2009). Characterization of antiplatelet properties of silver nanoparticles. *ACS Nano*, *3*(6), 1357-1364. https://doi.org/10.1021/nn900277t

Singh, J., & Dhaliwal, A. S. (2018). Plasmon-induced photocatalytic degradation of methylene blue dye using biosynthesized silver nanoparticles as photocatalyst. *Environmental Technology*, *41*(12), 1520-1534. https://doi.org/10.1080/09593330.2018.1540663

Timoteo, C. D. O., Paiva, R., Dos Reis, M. V., Claro, P. I. C., Ferraz, L. M., Marconcini, J. M., & de Oliveira, J. E. (2019). *In vitro* growth of *Physalis peruviana* L. affected by silver nanoparticles. *3 Biotech*, *9*, 1-9. https://doi.org/10.1007/s13205-019-1674-z

Vanaja, M., Paulkumar, K., Baburaja, M., Rajeshkumar, S., Gnanajobitha, G., Malarkodi, C., ... & Annadurai, G. (2014). Degradation of methylene blue using biologically synthesized silver nanoparticles. *Bioinorganic Chemistry and Applications*, *2014*, 1-8. https://doi.org/10.1155/2014/742346

Vidhu, V. K., & Philip, D. (2014). Catalytic degradation of organic dyes using biosynthesized silver nanoparticles. *Micron*, *56*, 54-62. https://doi.org/10.1016/j.micron.2013.10.006

Yisak, H., Yaya, E. E., Chandravanshi, B. S., & Redi-Abshiro, M. (2022). GC-MS profiling of fatty acids and nutritional properties of the white and brown teff [*Eragrostis tef* (Zuccagni) Trotter] varieties cultivated in different parts of Ethiopia. *Journal of Food Composition and Analysis*, *107*, 104405. https://doi.org/10.1016/j.jfca.2022.104405

Yukna, J. (2007). Computational and experimental investigations of the structural properties, electronic properties, and applications of silver, gold, mercury selenide, silver sulfide, and nickel sulfide nanoparticles. Southern Illinois University at Carbondale. 190 pages. https://books.google.co.in/books/about/Computational_and_Experimental_Investiga.html?id=cjb5SAAACAAJ&redir_esc=y

Zhu, F. (2018). Chemical composition and food uses of teff (*Eragrostis tef*). *Food chemistry*, *239*, 402-415. https://doi.org/10.1016/j.foodchem.2017.06.101